Inorg. Chem. **2002**, *41*, 7086–7093

New Oxovanadium Bis(1,2-dithiolate) Compounds That Mimic the Hydrogen-Bonding Interactions at the Active Sites of Mononuclear Molybdenum Enzymes

J. Jon A. Cooney, Michael D. Carducci, Anne E. McElhaney, Hugh D. Selby, and John H. Enemark*

Department of Chemistry, University of Arizona, Tucson, Arizona 85721-0041

Received July 8, 2002

Reaction of $VO(acac)_2$ with 1,2-dithiols in the presence of triethylamine gives pentacoordinate oxovanadium complexes $[HNEt_3]_2[VO(bdt)_2]$ (**1**), $[HNEt_3]_2[VO(tdt)_2]$ (**2**), and $[HNEt_3]_2[VO(bdtCl_2)_2]$ (**3**) (where H_2bdt = 1,2-benzenedithiol, H_2tdt = 3,4-toluenedithiol, and H_2bdtCl_2 = 3,6-dichloro-1,2-benzenedithiol). Compounds **1**–**3** have been characterized by IR, UV/visible, EPR, and mass spectroscopies. The X-ray crystal stuctures of **1** and **2** show hydrogen-bonding interactions between the terminal oxo atom and triethylammonium counterions and between ligand sulfur atoms and the counterions. These interactions are comparable with those found at the active sites of mononuclear molybdenum enzymes.

Introduction

Oxovanadium(IV) centers with two dithiolate ligands have received little attention since the first report in 1965.[1] However, interest in this type of $\{VOS_4\}$ center has increased with the evidence from recent collaborative studies by our group that *Azotobacter vinelandii* produces an alternative, vanadium-containing nitrate reductase (V-NR) that appears to be analogous to molybdenum-containing bacterial nitrate reductases.[2] Previous studies provided evidence for V-dependent nitrate reductase activity in cyanobacterium *Nostoc muscorum*[3] and *Psuedomonas isachenkovii*.[4,5] There are three types of bacterial NR: prokaryotic assimilatory NR (Nas); prokaryotic periplasmic NR (Nap); membrane-associated prokaryotic NR (Nar).[6] An example of dissimilatory Nap NR from *Desulfovibrio desulfuricans* has been crystallographically characterized and contains two pyranopterindithiolate moieties/metal atom.[7] *A. vinelandii* is in a subclade of organisms that produce Nas, whose structure is not yet known. If the vanadium site in V-NR is a direct analogue of that in Nap enzymes, then it too should possess bis(1,2-dithiolato) coordination. Analysis of protein sequence information reveals that 21 residues are conserved within the group of Nap enzymes examined that are associated with the binding of the two pyranopterindithiolate ligand molecules. In Nas enzymes, five residues that might be associated with ligand binding were identified, suggesting that perhaps only one pyranopterin ligand is associated with the metal atom. As yet there is no further evidence to support either structural motif for Nas enzymes.[6]

A common feature of all molybdenum enzymes possessing pyranopterindithiolate ligands is a network of hydrogen bonds that play an important role in anchoring the active site prosthetic group to the protein backbone residues.[8,9] This network maintains the orientation of the ligands relative to the metal atom, which may influence the redox potential of the active site.[8] The pyranopterin ligands have also been suggested to act as electron-transfer conduits.[8] In several cases, some of the ligand atoms at the metal center are hydrogen-bonded to the protein backbone. These "inner-coordination sphere" hydrogen bonds will have a direct effect

* To whom correspondence should be addressed. E-mail: jenemark@u.arizona.edu. Fax: (520) 626 8065.

(1) Atherton, N. M.; Locke, J.; McCleverty, J. A. *Chem. Ind.* **1965**, *7/17*, 1300.
(2) Cooney, J. J. A.; Joshi, H. K.; Codd, R.; Kennedy, C. K.; Enemark, J. H. *Abstracts of Papers*, 221st National Meeting of the American Chemical Society, San Diego, CA, 2001; American Chemical Society: Washington, DC, 2001; INOR-501.
(3) Singh, S.; Chakravarty, D.; Singh, H. N. *Biochem. Mol. Biol. Int.* **1993**, *29* (6), 1083−1093.
(4) Antipov, A. N.; Lyalikova, N. N.; Khiznjak, T. V.; L'vov N. P. *FEBS Lett.* **1998**, *441* (2), 257−260.
(5) Antipov, A. N.; Lyalikova, N. N.; Khiznjak, T. V.; L'vov N. P. *Biochemistry (Moscow)* **1999**, *64* (5), 483−487.
(6) Stolz, J. F.; Basu, P. *ChemBioChem* **2002**, *3* (2−3), 198−206.
(7) Dias, M. D.; Than, E. T.; Humm, A.; Huber. R.; Bourenkov, G. P.; Bartunik, H. D.; Bursakov, S.; Calvete, J.; Caldeira, C.; Moura, J. J. G.; Moura, I.; Romão, M. J. *Structure* **1999**, *7*, 65−79.
(8) Hille, R. In *Metal Ions in Biological Systems*; Sigel, A., Sigel, H., Eds.; Marcel Dekker: New York, 2002; pp 187−227.
(9) Stewart, L. J.; Bailey, S.; Bennett, B.; Charnock, J. M.; Garner, C. D.; McAlpine, A. S. *J. Mol. Biol.* **2000**, *299*, 593−600.

10.1021/ic025856e CCC: $22.00
Published on Web 12/05/2002

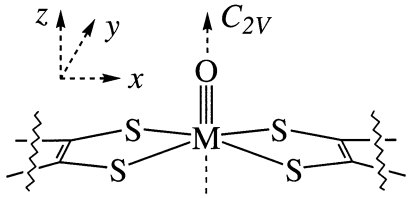

Figure 1. Coordinate system used for interpretation of the electronic absorption spectra of $[VO(bdt)_2]^{2-}$, $[VO(bdtCl_2)_2]^{2-}$, and related $[VOX_4]^{2-}$ complexes.

on the strengths of the metal−ligand bonds and, hence, affect the catalytic properties of the center. The crystal structures of SO[10] and DMSO reductase[11] also show hydrogen bonds to water molecules close to their molybdenum centers that support the catalytic cycles proposed for these enzymes.

An understanding of the chemistry and electronic structure of $\{VOS_4\}$ systems will provide important background information for interpreting the properties of V-NR. In addition, these investigations should provide complementary data for understanding the mode-of-action of pyranopterin active sites in enzymes. Analysis of the electronic structure of $\{VOS_4\}$ systems follows those for $[MOX_4]^{n-}$ (M = V, n = 2; M = Cr, Mo, W, n = 1; X = F, Cl, Br) and $[MoOS_4]^-$ [$S_4 = (SPh)_4$, $(bdt)_2$, $(S_2C_2H_4)_2$] that have been built up from solution, powder, and single-crystal EPR, UV/vis absorption, and MCD spectroscopic studies.[12−14] In pseudotetragonal symmetry the electronic structure is dominated by the oxo−metal bond, resulting in a $d_{x^2-y^2} < d_{xz} \approx d_{yz} < d_{xy} < d_{z^2}$ energy ordering for the d orbitals. (The C_{2v} coordinate system of Figure 1 has been chosen to facilitate comparison among all the VOS_4 compounds.) In $[MoOS_4]^-$ complexes LMCT can occur to the metal d orbitals from the filled and essentially nonbonding ligand orbitals that are localized on the equatorial donor atoms.[15−17]

Oxovanadium bis(dithiolates) are part of a larger family of vanadium dithiolate compounds. This family also includes vanadium tris(dithiolate) compounds, e.g., $[NEt_4]_2[V(bdt)_3]$,[18] vanadocene dithiolate compounds, e.g., $(Cp)_2V(bdt)$,[19] and clusters, e.g., $[\{V(bdt)_2O\}_2V(tmeda)_2]$[20] (where H_2bdt = 1,2-benzenedithiol, HCp = cyclopentadiene, and tmeda = *N*,*N*,*N*′,*N*′-tetramethylethylenediamine). Herein, we report the synthesis and characterization of $[HNEt_3]_2[VO(bdt)_2]$ (**1**), $[HNEt_3]_2[VO(tdt)_2]$ (**2**), and $[HNEt_3]_2[VO(bdtCl_2)_2]$ (**3**) (where H_2tdt = 3,4-toluenedithiol and H_2bdtCl_2 = 3,6-dichloro-1,2-benzenedithiol; Figure 2).

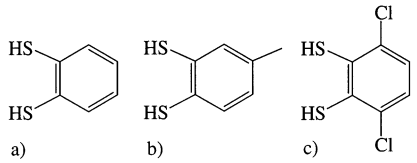

Figure 2. Representation of (a) H_2bdt = 1,2-benzenedithiol, (b) H_2tdt = 3,4-toluenedithiol, and (c) H_2bdtCl_2 = 3,6-dichloro-1,2-benzenedithiol.

Experimental Section

All syntheses were carried out under anaerobic conditions using standard glovebox techniques. MeCN was distilled from CaH_2; THF, Et_2O, and hexanes were distilled from NaK/benzophenone, and triethylamine was distilled from NaK. All solvents were thoroughly degassed by freeze, pump, thaw cycling three times. H_2bdt, H_2tdt, and H_2bdtCl_2 were used as received (Aldrich). IR spectra were recorded as KBr disks using a Nicolet Avatar 360 FTIR spectrometer. The X-ray crystallographic structures were determined by the Molecular Structure Laboratory at the University of Arizona. UV/vis spectra were recorded using an OLIS Cary 14 spectrophotometer. The X-band (∼9.1 GHz) EPR spectra were obtained on a Bruker ESP 300 spectrometer, and mass spectra were recorded on a JEOL HX110 high-resolution sector instrument at the facilities at the University of Arizona.

Cyclic voltammetric (CV) data were collected on a Bioanalytical Systems (BAS) CV-50W system. BAS-supplied software provided scan acquisition control and data analysis/graphics capabilities. The electrochemical cell employed was based on a normal three-electrode configuration. This cell consists of a platinum disk working electrode (1.6 mm diameter, BAS), a platinum wire counter electrode (BAS), and a NaCl-saturated Ag/AgCl reference electrode (BAS). Prior to each experiment, the electrode was polished using 0.05 mm alumina (Buehler) and electrochemically cleaned in dilute sulfuric acid. Cyclic voltammetric measurements were performed in dry chloroform solutions (10 mL, 25 °C) over a potential window of +200 to −400 for **1**, +300 to −500 for **2**, and +600 to −400 mV vs Ag/AgCl for **3** with 0.1−0.2 M dried tetra-*n*-butylammonium tetrafluoroborate $[n\text{-}Bu_4N][BF_4]$ (Aldrich) as the supporting electrolyte. The background scans of dry chloroform with the $[n\text{-}Bu_4N][BF_4]$ supporting electrolyte exhibited no electroactive impurities or solvent decomposition within the potential window employed.

General Procedure for the Preparation of $[HNEt_3]_2[VO(dt)_2]$ [dt = bdt (1), tdt (2), and $bdtCl_2$ (3)]. To a suspension of $VO(acac)_2$ (0.132 g, 0.55 mmol) in a mixture of 1,1-dichloroethane (35 mL) and NEt_3 (5 mL), the 1,2-dithiol (1.0 mmol) was added. The mixture was allowed to stir for 30 min. The precipitate was removed by filtration and washed with ether (2 × 5 mL). The green solid was then allowed to dry. Recrystallization of **1** and **2** by vapor diffusion of Et_2O into a solution of the compound in MeCN at −30 °C yielded brown rod-shaped crystals suitable for crystallography. Recrystallization of **3** by the same technique yielded a brown crystalline solid.

$[HNEt_3]_2[VO(bdt)_2]$ (1). Yield: 0.142 g (51.5%). UV/vis [in MeCN; λ, cm^{-1} (ϵ, M^{-1} cm^{-1})]: 11 300 (36), 17 400 (244), 19 700 (142), 22 600 (714). IR (KBr disk, cm^{-1}): ν(V≡O) 903. ESI MS (*m*/*z*): 347, $[VO(bdt)_2]^-$; 678, $[O\{V(bdt)_2\}_2]^-$; 795, $\{[HNEt_3][VO(bdt)_2]_2\}^-$.

$[HNEt_3]_2[VO(tdt)_2]$ (2). Yield: 0.124 g (42.8%). UV/vis [in MeCN; λ, cm^{-1} (ϵ, M^{-1} cm^{-1})]: 10 600 (278), 17 100 (329), 19 800 (208), 22 200 (929). IR (KBr disk, cm^{-1}): ν(V≡O) 906. ESI MS

(10) Kisker, K.; Schindelin, H.; Pacheco, A.; Wehbi, W. A.; Garrett, R. M.; Rajagopalan, K. V.; Enemark, J. H.; Rees, D. C. *Cell* **1997**, *91*, 973−983.
(11) McAlpine, A. S.; McEwan, A. G.; Shaw, A. L.; Bailey, S. *JBIC, J. Biol. Inorg. Chem.* **1997**, *2*, 690−701.
(12) Garner, C. D.; Hill, L. H.; Mabbs, F. E.; McFadden, D. L.; McPhail, A. T. *J. Chem. Soc., Dalton Trans.* **1977**, 1202−1207.
(13) Gray, H. B.; Hare, C. *Inorg. Chem.* **1962**, *1*, 363−368.
(14) Collison, D. *J. Chem. Soc., Dalton Trans.* **1990**, 2999−3006.
(15) McMaster, J.; Carducci, M. D.; Yang, Y.-S.; Solomon, E. I.; Enemark, J. H. *Inorg. Chem.* **2001**, *40*, 687−702.
(16) McNaughton, R. L.; Helton, M. E.; Rubie, N. D.; Kirk, M. L. *Inorg. Chem.* **2000**, *39*, 4386−4387.
(17) Carducci, M. D.; Brown, C.; Solomon, E. I.; Enemark, J. H. *J. Am. Chem. Soc.* **1994**, *116*, 11856−11868.
(18) Kondo, M.; Minakoshi, S.; Iwata, K.; Shimizu, T.; Matsuzaka, H.; Kamigata, N.; Kitagawa, S. *Chem. Lett.* **1996**, 489−490.
(19) Stephan, D. W. *Inorg. Chem.* **1992**, *31*, 4218−4223.
(20) Tsagkalidis, W.; Rodewald, D.; Rehder, D. *J. Chem. Soc., Chem. Commun.* **1995**, *2*, 165−166.

Table 1. X-ray Crystallographic Parameters for **1** and **2**

param	**1**	**2**
empirical formula	$C_{24}H_{40}N_2OS_4V$	$C_{26}H_{44}N_2OS_4V$
fw	551.76	579.81
temp (K)	173(2)	110(2)
wavelength (Å)	0.710 73	0.710 73
cryst system	orthorhombic	orthorhombic
space group	*Fdd*2	*Fdd*2
unit cell dimens (Å)	$a = 26.3233(19)$	$a = 27.480(9)$
	$b = 26.9947(19)$	$b = 27.749(9)$
	$c = 7.9574(6)$	$c = 7.847(2)$
V (Å^3)	5654.4(7)	5984(3)
Z	8	8
D(calcd) (Mg/m^3)	1.296	1.287
abs coeff (mm^{-1})	0.665	0.632
reflcns utilized	14 548	11 522
indpdt reflcns	2989 [R(int) = 0.0771]	3079 [R(int) = 0.0466]
final R indices	$R_1 = 0.0466$,	$R_1 = 0.0421$,
$[I > 2\sigma(I)]$	$wR_2 = 0.0977$[a]	$wR_2 = 0.0926$[b]
R indices	$R_1 = 0.1073$,	$R_1 = 0.0554$,
(all data)	$wR_2 = 0.1117$[a]	$wR_2 = 0.0993$[b]

[a] $R_1 = \sum||F_o| - |F_c||/\sum|F_o|$, $wR_2 = \{\sum[w(F_o^2 - F_c^2)^2]/\sum[w(F_o^2)^2]\}^{1/2}$, $w = 1/[\sigma^2(F_o^2) + (0.0479P)^2]$, where $P = (F_o^2 + 2F_c^2)/3$. [b] $w = 1/[\sigma^2(F_o^2) + (0.0538P)^2 + 2.1134P]$.

(m/z): 375, $[VO(tdt)_2]^-$; 734, $[O\{V(tdt)_2\}_2]^-$; 851, $\{[HNEt_3][VO(tdt)_2]_2\}^-$; 954, $\{[HNEt_3]_2[VO(tdt)_2]_2\}^-$.

$[HNEt_3]_2[VO(bdtCl_2)_2]$ (3). Yield: 0.123 g (35.8%). UV/vis [in MeCN; λ, cm^{-1} (ϵ, M^{-1} cm^{-1})]: 11 700 (31), 17 800 (264), 20 600 (137), 23 250 (774). IR (KBr disk, cm^{-1}): ν(V≡O) 917. ESI MS (m/z): 347, $[VO(bdtCl_2)_2]^-$; 953, $[O\{V(bdtCl_2)_2\}_2]^-$.

X-ray Crystallographic Analysis. Data were collected for **1** and **2** on a Bruker SMART 1000 CCD detector X-ray diffractometer. Data collection parameters are summarized in Table 1. The structure was solved using SHELXS in the Bruker SHELXTL (version 5.0) software package.[21] Refinements were performed using SHELXL and illustrations were made using XP. Solution was achieved utilizing direct methods followed by Fourier synthesis. For both **1** and **2**, the ammonium hydrogen atom was located in difference maps which did not include the idealized atom. Once located, the hydrogen atom was allowed to refine freely. The remaining hydrogen atoms were added at idealized positions, constrained to ride on the atom to which they are bonded and given thermal parameters equal to 1.2 or 1.5 times U_{iso} of that bonded atom. In **2**, the tdt^{2-} ligand was found to be disordered as evidenced by significant residual electron density at both the 4 and 5 positions of the benzene ring. These two sites were modeled as parts of the same disordered methyl group and were given initial occupancies of 0.5. The relative occupancies of the two sites were then allowed to refine as a free variable, yielding final occupancies of 59.08(6)% for C7 and 40.09(6)% for C8. The final anisotropic full-matrix least-squares refinement based on F^2 of all reflections converged (maximum shift/esd = 0.000) for **1** at $R_1 = 0.1073$, $wR_2 = 0.1117$, and goodness-of-fit = 0.864 and for **2** at $R_1 = 0.055$, $wR_2 = 0.099$, and goodness-of-fit = 1.053. "Conventional" refinement indices using the 1564 reflections with $F > 4\sigma(F)$ are $R_1 = 0.047$ and $wR_2 = 0.098$ for **1** and $R_1 = 0.042$ and $wR_2 = 0.093$ for **2** using the 2621 reflections with $F > 4\sigma(F)$.

Theoretical Methods. The electronic structures of the $[VO(bdt)_2]^{2-}$ and $[VO(bdtCl_2)_2]^{2-}$ anions were investigated using the Amsterdam Density Functional (ADF version 2000.01) program package.[22−25] The program implements numerical integration in Cartesian space,[24] and gradients for geometry optimizations are solved analytically.[23] The optimizations of $[VO(bdt)_2]^{2-}$ and $[VO(bdtCl_2)_2]^{2-}$ were performed with the anions in C_{2v} geometry. Because of the symmetry restrictions, the optimized geometry does not necessarily represent a minimum on the respective potential energy surface for the gas-phase structure. In the gas phase, the lowest energy structure will maximize intramolecular hydrogen bonding, which is not evident in these systems. In condensed phase systems, however, hydrogen bonding will occur with surrounding solvent molecules and, as is evident in the crystal structures, with counterions. Optimized structures obtained without including solvent effects but with symmetry constraints will be used throughout this paper. This will allow a systematic study of the impact of the structure of the complex and the identity of the ligands on the calculated parameters.

Scalar relativistic effects were included in all calculations using the zero-order regular approximation (ZORA).[26−29] The relativistic atomic potentials necessary for each atom were calculated using the auxiliary program DIRAC, which is supplied with the ADF program package. The density functional for all calculations used a generalized gradient approximation with the exchange correction of Becke[30] and the correlation correction of Lee et al.[31] Each molecule studied contained one unpaired electron; therefore, all calculations were performed both in the spin-restricted and -unrestricted mode. Estimates of transition energies were made using the Slater transition state formalism in which the energy of an electronic transition is determined by the orbital-energy difference from a stationary-point calculation where the population of the ground-state molecular orbital (MO) is lowered by 0.5 and the population of the excited-state MO is increased by 0.5.[32] For spin-unrestricted calculations the occupancies of the MO's were chosen to have overall α-spin.

Results and Discussion

Crystallographic Studies. The complex anions of **1** and **2** adopt pseudo square pyramidal geometry and contain two dithiolate ligands equatorially bound via their sulfur atoms to an axial oxovanadium group [see Figure 3 and Figure S1 (Supporting Information)]. The anions have crystallographically imposed C_2 symmetry. The asymmetric unit of **1** contains the oxovanadium unit, one of the dithiolate ligands, and a single triethylammonium counterion; the remaining atoms are generated by the 2-fold rotation axis along the VO bond vector. The triethylammonium counterions are disposed about the oxo oxygen such that they lie above one side of each sulfur-containing ligand. This arrangement allows for close H-bonding to the oxo oxygen via the ammonium proton as well as to one of the sulfur atoms (S1) of the dithiolate ligands. The asymmetric unit of **2** is very similar to that of **1**; however, the tdt^{2-} ligand possesses a

(21) Bruker. *SHELXTL Reference Manual Version 5.0*; Bruker AXS Inc.: Madison, WI, 1997.
(22) Baerends, E. J.; Ellis, D. E.; Ros, P. *Chem. Phys.* **1973**, *2*, 41−51.
(23) Versluis, L.; Ziegler, T. *J. Chem. Phys.* **1988**, *88*, 322.
(24) te Velde, G.; Baerends, E. J. *J. Comput. Phys.* **1992**, *99* (1), 84−98.
(25) Fonseca Guerra, C.; Snijders, J. G.; te Velde, G.; Baerends, E. J. *Theor. Chem. Acc.* **1998**, *99*, 391.
(26) van Lenthe, E.; Baerends, E. J.; Snijders, J. G. *J. Chem. Phys.* **1994**, *101*, 9783.
(27) van Lenthe, E.; Snijders, J. G.; Baerends, E. J. *J. Chem. Phys.* **1996**, *105*, 6505.
(28) van Lenthe, E.; Leeuwen, R. v.; Baerends, E. J.; Snijders, J. G. *Int. J. Quantum Chem.* **1996**, *57*, 281.
(29) van Lenthe, E.; Ehlers, A. E.; Baerends, E. J. *J. Chem. Phys.* **1999**, *110*, 8943.
(30) Becke, A. D. *Phys. Rev. A* **1988**, *38*, 3098−3100.
(31) Lee, C.; Yang, W.; Parr, R. G. *Phys. Rev. B* **1988**, *37*, 785.
(32) Slater, J. C. *Adv. Quantum. Chem.* **1972**, *6*, 1−92.

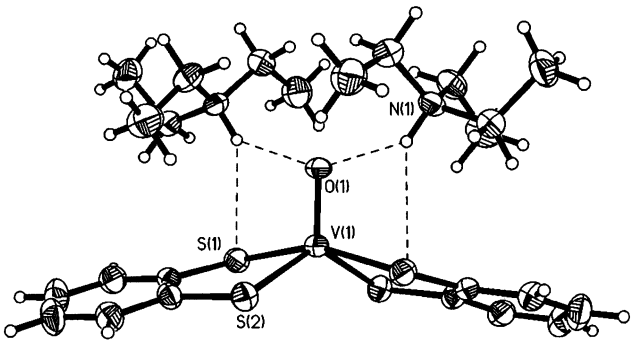

Figure 3. ORTEP representation of **1** with thermal ellipsoids depicted at the 50% probability level. Hydrogen atoms are shown as small spheres for clarity.

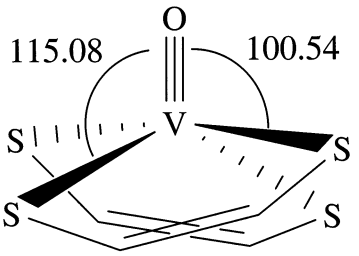

Figure 4. Illustration of the vanadium center of **1** highlighting the difference in the O−M−S angles, which demonstrates the deviation from coplanarity of the four sulfur ligands.

methyl group that is disordered over two sites, C4 and C5, in ca. 60/40 occupancy ratio. The second ligand is generated by a 2-fold rotation, as in **1**. The presence of the methyl group implies the existence of different isomers. However, the C_2 axis of symmetry generating the second tdt^{2-} ligand prohibits identification of the isomers. The disorder allows for the presence of anions which are not C_2 symmetric in a C_2 symmetric space group; hence, the two ligands may be present with the methyl groups cis or trans to each other.

The five ligand atoms of the $\{VOS_4\}$ group form an approximate square-based pyramid. However, the four sulfurs in the basal plane are twisted away from being coplanar, resulting in a lowering of symmetry from C_{2v} to C_2. This twist can be seen in the difference in the O−M−S angles (Table 2) within the anion (14.54° for **1** and 14.44° for **2**; see Figure 4). The structures of **1** and **2** can be compared with the structures reported for similar complexes (see Table 2).[33−35] The smaller differences in the O−M−S angles (<7°) in the other reported complexes imply that their ligand S atoms are more nearly coplanar. The reasons for the twist away from coplanarity in **1** and **2** may include the H-bonding interaction between one of the S atoms in each ligand and the N−H ammonium proton (**1**, S−H = 2.64(5), S−N = 3.491(5) Å; **2**, S−H = 2.62(4), S−N = 3.388(3) Å), as shown in Figure 3. The structure of the anions in **1** and **2** are similar to that of the $\{V(bdt)_2O\}$ unit in $[\{V(bdt)_2O\}_2V(tmeda)_2]$;[20] however, the V−O bond length in $[\{V(bdt)_2O\}_2V(tmeda)_2]$ is longer, as would be expected for a V−O−V unit. The ligand S atoms are more nearly coplanar in the $\{V(bdt)_2O\}$unit, with O−M−S angles of 105.5(2), 112.1(2), 105.0(2), and 113.2(2)°.

Table 2. Selected Bond Lengths and Angles for **1**, **2**, and Analogous Complex Anions[20,33−35]

anion	M−O (Å)	M−S (Å)	O−M−S (deg)
$[VO(bdt)_2]^{2-}$ (anion of **1**)	1.639(4)	2.3448(14) 2.3668(13)	115.08(5) 100.54(4)
$[VO(tdt)_2]^{2-}$ (anion of **2**)	1.628(3)	2.3543(10) 2.3848(10)	114.73(3) 100.29(3)
$[VO(mnt)_2]^{2-}$ [33]	1.579(10)	2.356(4), 2.407(3) 2.372(3), 2.360(3)	103.7(4), 104.9(4) 103.1(4), 104.0(0)
[VO(dithiosquarate)$_2$]$^{2-}$ [34]	1.595(4)	2.453(8), 2.506(8) 2.450(8), 2.402(6)	104.1(3), 105.0(3) 106.0(3), 104.9(3)
$[\{V(bdt)_2O\}_2V(tmeda)_2]$[20]	1.668(6)	2.377(3), 2.334(3) 2.367(3), 2.343(3)	105.5(2), 112.1(2) 105.0(2), 113.2(2)
$[MoO(bdt)_2]^{2-}$ [35]	1.700(6) 1.694(6)	2.3913(19), 2.3843(19) 2.3874(19), 2.3787(19)	106.95(5), 109.41(5) 108.70(5), 107.86(5)

The H-bonding interaction between the oxo atom and the triethylammonium counterion (**1**, O−H = 2.15(4), O−N = 2.882(5) Å; **2**, O−H = 2.23(3), O−N = 2.904(3) Å) may account for the slightly longer V≡O bond length for **1** (1.639(4) Å) and **2** (1.628(3) Å) compared to the analogous maleonitriledithiolato (1.579(10) Å) and dithiosquarato (1.595(4) Å) complexes.[33,34] Other compounds have shown that the thiolate S atoms can be hydrogen bonded to counterions; in triethylammonium oxomolybdenum bis(biphenyl-2,2′-dithiolate), one of the sulfur ligand atoms is hydrogen bonded to the counterion.[36] It is interesting that the hydrogen-bonding interactions of the vanadium centers of **1** and **2** mimic those found in molybdenum- and tungsten-containing enzymes. Both the terminal oxo group and ligand sulfur atoms of the vanadium-containing anion are hydrogen bonded to the proton of the countercation. Similar interactions involving terminal metal−oxo and ligand sulfur atoms and less acidic hydrogen bond donors of the protein occur at the active sites of several pyranopterin-containing enzymes. For example, hydrogen bonds that involve the sulfur ligand atoms of the pyranopterindithiolate ligand groups occur in *D. desulfuricans* Nap (to His623)[7] and in both the oxidized and reduced forms of *E. coli* formate dehydrogenase H (to Gln335).[37]

The terminal ligands of the molybdenum center are also found to be involved in hydrogen bonding including the oxo atom in chicken liver sulfite oxidase (to Trp116 and to a water molecule).[10] Similar interactions occur at the active sites of *R. sphaeroides*[38,39] and *R. capsulatus* DMSO reductase,[9,11,40−42] *Shewanella massilia* trimethylamine *N*-

(33) Collison, D.; Mabbs, F. E.; Temperley, J.; Christou, G.; Huffman, J. C. *J. Chem. Soc., Dalton Trans.* **1988**, 309−314.
(34) Wenzel, B.; Strauch, P. *Z. Naturforsch.* **1999**, *54b*, 165−170.
(35) Boyde, S.; Ellis, S. R.; Garner, C. D.; Clegg, W. *J. Chem. Soc., Chem. Commun.* **1986**, 1541−1543.
(36) Conry, R. R.; Tipton, A. A. *J. Biol. Inorg. Chem.* **2001**, *6*, 359−366.
(37) Boyington, J. C.; Gladyshev, V. N.; Khangulov, S. V.; Stadtman, T. C.; Sun, P. D. *Science* **1997**, *275*, 1305−1308.
(38) Schindelin, H.; Kisker, C.; Hilton, J.; Rajagopalan, K. V.; Rees, D. C. *Science* **1996**, *272*, 1615−1621.
(39) Li, H.-K.; Temple, C.; Rajagopalan, K. V.; Schindelin, H. *J. Am. Chem. Soc.* **2000**, *122*, 7673−7680.
(40) Schneider, F.; Löwe, J.; Huber, R.; Schindelin, H.; Kisker, C.; Knäblein, J. *J. Mol. Biol.* **1996**, *263*, 53−69.
(41) Bray, R. C.; Adams, B.; Smith, A. T.; Bennett, B.; Bailey, S. *Biochemistry* **2000**, *39*, 11258−11269.
(42) McAlpine, A.; McEwan, A.; Bailey, S. *J. Mol. Biol.* **1998**, *275*, 613−623.

oxide reductase,[43] and *D. gigas* aldehyde oxidoreductase.[44] The thio atom in *R. capsulatus* xanthine dehydrogenase[45] is found to be hydrogen bonded to the peptide backbone (Gln197). A further type of hydrogen bonding is demonstrated in *E. coli* formate dehydrogenase H, where the selenium ligand atom of the selenocysteine bound to the molybdenum atom interacts with His141.[37]

Cyclic Voltammetric Studies. The cyclic voltammograms of **1**−**3** show a reversible one-electron oxidation couple ($E_{1/2}$ = −84.7, −112.5, and 117.5 mV vs Ag/AgCl, respectively) in chloroform solution (25 °C), assigned as a V^{V}/V^{IV} couple. The chemical reversibility determined by peak current ratios are near unity ($i_{pa}/i_{pc} \approx 1.0$), and the peak currents are proportional to the square root of the scan rate. The reversibility of the oxidation couples indicates that minimal structural rearrangement occurs during the electrochemical processes. The dependence of $E_{1/2}$ upon the nature of the dithiolate ligand is in the order $tdt^{2-} < bdt^{2-} < bdtCl_2^{2-}$. This ordering is the same as that seen for the Mo^{VI}/Mo^{V} and the Mo^{V}/Mo^{IV} couples of $[(Tp^*)MoO(dt)]^{0/+}$ (where Tp* is hydrotris(3,5-dimethyl-1-pyrazolyl)borate) with the same ligands.[46] The range of 202 mV for the V^{V}/V^{IV} couple for these ligands compares to ranges of 280 and 140 mV for the Mo^{VI}/Mo^{V} and the Mo^{V}/Mo^{IV} couples, respectively. The redox potential data of the molybdenum− and vanadium−dithiolate complexes show that the ease of reduction and difficulty in oxidation increases as the 1,2-dithiolate ligand becomes increasingly more electron-withdrawing. A further irreversible oxidation process is observed for **3** at ∼1258 mV vs Ag/AgCl. A similar process is also observed for **1** and **2**; however, it is at ∼1500 mV vs Ag/AgCl and hence not readily studied in chloroform, due to a process involved with the decomposition of the solvent.

Spectroscopic Studies. The IR spectra of **1**−**3** showed bands at around 900 cm^{-1} [KBr disks (cm^{-1}): **1**, 903; **2**, 906; **3**, 917 cm^{-1}. $CHCl_3$ solution (cm^{-1}): **1**, 904; **2**, 900]. These frequencies are lower than the expected 935−1035 cm^{-1} reported for V≡O for a large set of oxovanadium complexes.[47,48] The lowering of these frequencies is due to the fact that the oxo atom is H-bonded to the two ammonium cations thereby weakening the V≡O bond. Mass spectrometric results showed the presence of the dianion as a salt with the counterion, e.g. $\{[HNEt_3]_2[VO(dt)_2]_2\}$, and that the dianions underwent transformations in the spectrometer resulting in the formation of the monoanionic species and O atom bridged dimers, e.g. $\{(dt)_2VOV(dt)_2\}$.

The electronic structures of oxovanadium (V≡O) complexes have been of interest since the seminal work of Ballhausen and Gray.[49] Subsequent work by Collison et al.[50]

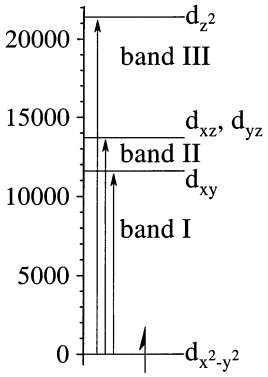

Figure 5. Proposed assignment of the electronic transitions of $[NEt_4]_2[VOCl_4]$ (adapted from Collison et al).[50] The orbital labels are those for C_{2v} symmetry (Figure 1) to facilitate comparison to the VOS_4 complexes.

based on low-temperature single-crystal polarized electronic absorption spectroscopy of oxovanadium complexes used the assignment of bands I, II, and III for $d_{x^2-y^2} \rightarrow d_{xy}$, $d_{x^2-y^2} \rightarrow d_{xz}$,$d_{yz}$, and $d_{x^2-y^2} \rightarrow d_{z^2}$, respectively. For complexes of the type $[VOX_4]^{2-}$ (X = Cl and NCS) and $[VOX_2Y_2]$ (X = Cl and Br; Y = tetramethylurea, tetramethylthiourea, hexamethylphosphoramide, and triphenylphosphine oxide) this work showed that the order of bands was I < II ≪ III (see Figure 5) implying that $d_{x^2-y^2}$ was the HOMO and the energy of the orbitals increased in the order $d_{x^2-y^2} < d_{xy} < d_{xz} \approx d_{yz} < d_{z^2}$. (The geometries of these oxovanadium and $[MoOL_4]^-$ complex anions are close to C_{4v} or C_{2v} symmetry. For convenience, the metal d orbitals have been labeled using the C_{2v} coordinate system of Figure 1.)

Bands I and II are shown to be close together (within ∼3000 cm^{-1}) in energy. Band III was at higher energy (∼6000 cm^{-1} higher) and distinct from bands I and II. The fact that these spectra are similar to each other, despite changes in the equatorial ligation, supports the theory of the dominance of the V≡O bond over the ligand-field manifold.

The transitions of $[VO(mnt)_2]^{2-}$ (mnt = maleonitriledithiolate) have been assigned by Atherton and Winscom:[51] the lowest energy transition at 10 500 cm^{-1} as type II $[d_{x^2-y^2}(a_1) \rightarrow d_{xz}(b_1), d_{yz}(b_2)]$; the transition at 17 400 cm^{-1} as type I $[d_{x^2-y^2} \rightarrow d_{xy}(a_2)]$; the band at 25 600 cm^{-1} as MLCT $[V\ d_{x^2-y^2} \rightarrow S_2\ 3p_z + C_2\ 2p_z\ \pi(b_2)]$. The band at 25 600 cm^{-1} was reassigned as type III $[d_{x^2-y^2} \rightarrow d_{z^2}]$ by Collison et al.[33] However, both these assignments imply a difference in energy between bands I and II of ∼7000 cm^{-1} in contrast with that of other VOX_4 and VOX_2Y_2 complexes. Three absorption bands are reported for $[NEt_4]_2[VO(bdtCl_4)_2]$ ($bdtCl_4$ = 3,4,5,6-tetrachloro-1,2-benzenedithiolate)[52] and are at energies similar to those of $[VO(mnt)_2]^{2-}$. The electronic absorption spectrum of $[PPh_4]_2[VO(qdt)_2]$ (qdt = quinoxalinedithiolate)[53] recorded as a barium sulfate disk shows three absorption bands at energies to similar those of $[VO(mnt)_2]^{2-}$

(43) Czjzek, M.; Dos Santos, J.-P.; Pommier, J.; Giordano, G.; Méjean, V.; Haser, R. *J. Mol. Biol.* **1998**, *284*, 435−447.
(44) Romão, M. J.; Archer, M.; Moura, I.; Moura, J. J. G.; LeGall, J.; Engh, R.; Schneider, M.; Hof, P.; Huber, R. *Science* **1995**, *270*, 1170−1176.
(45) Truglio, J. J.; Theis, K.; Leimkühler, S.; Rappa, R.; Rajagopala, K. V.; Kisker, C. *Structure* **2001**, *10*, 1−20.
(46) Inscore, F. E.; Joshi, H. K.; McElhaney, A. E.; Enemark, J. E. *Inorg. Chim. Acta* **2002**, *331*, 246−256.
(47) Selbin, J. *Chem. Rev.* **1965**, *65*, 153−175.
(48) Selbin, J. *Coord. Chem. Rev.* **1966**, *1*, 293−314.
(49) Ballhausen, C. J.; Gray, H. B. *Inorg. Chem.* **1962**, *1* (1), 111−122.
(50) Collison, D.; Gahan, B.; Garner, C. D.; Mabbs, F. E. *J. Chem. Soc., Dalton Trans.* **1980**, 667−674.
(51) Atherton, N. M.; Winscom, C. J. *Inorg. Chem.* **1972**, *12* (2), 383−390.
(52) McCleverty, J. A.; Locke, J.; Ratcliff, B.; Wharton, E. J. *Inorg. Chim. Acta* **1969**, *3* (2), 283−286.
(53) Mabbs, F. E.; Temperley, J. *Spectrochim. Acta* **1989**, *45A* (2), 285−291.

Table 3. Electronic Absorption Data for **1**−**3** and Selected $[VO(dt)_2]^{2-}$-Containing Compounds[52,53]

anion	λ, cm^{-1} (ϵ, M^{-1} cm^{-1})				solvent
$[VO(bdt)_2]^{2-}$ (anion of **1**)	11 300 (36)	17 400 (244)	19 700 (142)	22 600 (714)	MeCN
$[VO(tdt)_2]^{2-}$ (anion of **2**)	10 600 (278)	17 100 (329)	19 800 (208)	22 200 (929)	MeCN
$[VO(bdtCl_2)_2]^{2-}$ (anion of **3**)	11 700 (31)	17 800 (264)	20 600 (137)	23 250 (774)	MeCN
$[VO(mnt)_2]^{2-}$ [52]	10 500 (170)	17 400 (380)		26 400 (2160)	DCM
$[VO(bdtCl_4)_2]^{2-}$ [52]	11 900 (4)	18 300 (65)		23 400 (520)	DCM
$[VO(qdt)_2]^{2-}$ [53,a]	13 160 (0.15)	18 180 (0.22)	20 730 (0.26)	24 120 (0.35)	

[a] Values in parentheses are relative intensities, recorded as a $BaSO_4$ disk.

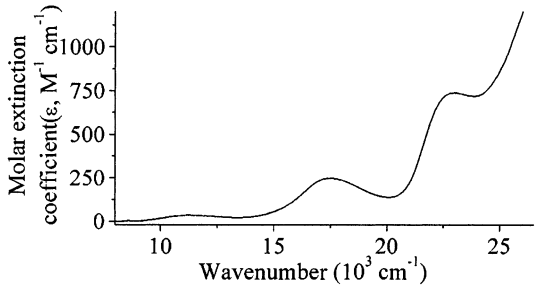

Figure 6. Electronic absorption spectrum for **1** in MeCN at 298 K.

and a fourth band at 20 730 cm^{-1}, assigned to $d_{x^2-y^2} \rightarrow d_{z^2}$. The similarity of the electronic absorption spectra of these $[VO(dithiolate)_2]^{2-}$ complexes implies that the electronic structure of the $\{VOS_4\}$ center is maintained despite changes in the nature of the dithiolate ligand.

The electronic absorption spectra of **1**−**3** are very similar to one another and show three broad absorptions at ∼11 000, ∼17 500, and ∼23 000 cm^{-1} in MeCN (Figure 6) that are at similar energies to those for $[PPh_4]_2[VO(mnt)_2]$ (see Table 3).[1,33,51] These bands can be fit with four Gaussian functions (Table 3), and the energy of the fourth weak overlapping band (∼20 000 cm^{-1}) is comparable with that found for $[VO(qdt)_2]^{2-}$.[53] These absorptions are followed by the onset of an intense charge-transfer feature above ∼25 000 cm^{-1} (Figure 6).

Comparison of the electronic absorption spectra of the VO^{2+} and MoO^{3+} chromophores has led to useful assignments of spectral features.[14,54] The electronic absorption spectrum of $[PPh_4][MoO(bdt)_2]$ shows[16] absorption bands at 19 400 and 13 700 cm^{-1} assigned as LMCT bands. The band at 13 700 cm^{-1} is assigned as S p_x(nonbonding) → Mo $d_{x^2-y^2}$ and that at 19 400 cm^{-1} as S p_x(bonding) → Mo $d_{x^2-y^2}$, where the p_x orbitals are in-plane with the dithiolate ligand. A further band observed at 12 000 cm^{-1} in $\{MoOS_4\}$ complexes has been assigned as S p_π(nonbonding) → Mo $d_{x^2-y^2}$.[55]

The band at ∼11 000 cm^{-1} in the absorption spectra of $[VO(dithiolate)_2]^{2-}$ complexes can be assigned to S $p_\pi \rightarrow$ V $d_{x^2-y^2}$ from comparison with the spectrum of $[MoO(bdt)_2]^-$. The band at ∼17 500 cm^{-1} can be assigned as three overlapping bands $d_{x^2-y^2} \rightarrow d_{xy}$, d_{xz}, and d_{yz}, that at ∼20 000 cm^{-1} as $d_{x^2-y^2} \rightarrow d_{z^2}$, and that at ∼23 000 cm^{-1} as an MLCT band of type V $d_{x^2-y^2} \rightarrow S_2\ 3p_z + C_2\ 2p_z$ (b_2). This assignment is consistent with that of $[VOCl_4]^{2-}$ in that the bands $d_{x^2-y^2} \rightarrow d_{xy}$, d_{xz}, and d_{yz} are close together in energy. However, in the absorption spectra of $[VO(dithiolate)_2]^{2-}$ complexes, the band at ∼11 000 cm^{-1} is very weak for a charge-transfer transition, with absorption coefficient (ϵ) < 300 M^{-1} cm^{-1} and usually < 50 M^{-1} cm^{-1}.

Alternatively, from comparison with the spectrum of $[VOCl_4]^{2-}$, the band at ∼11 000 cm^{-1} in the absorption spectra of $[VO(dithiolate)_2]^{2-}$ complexes can be assigned to $d_{x^2-y^2} \rightarrow d_{xy}$. In $[MO(bdt)_2]^{n-}$ compounds (where M = V, n = 2, and M = Mo, n = 1), the transition $d_{x^2-y^2} \rightarrow d_{xy}$ is equivalent to 10*Dq* for an octahedral complex. Therefore, the position of this band with different equatorial ligand sets should parallel the spectrochemical series. Sulfur donors are generally weaker ligand than chloride, and thus, the transition should occur below 13 000 cm^{-1}, the value observed for $[VOCl_4]^{2-}$. The other bands in the spectra of $[VO(dithiolate)_2]^{2-}$ are assigned as the following: that at ∼17 500 cm^{-1} to $d_{x^2-y^2} \rightarrow d_{xz}$, d_{yz}; that at ∼20 000 cm^{-1} to $d_{x^2-y^2} \rightarrow d_{z^2}$; that at ∼23 000 cm^{-1} to an MLCT band. The transition $a_1 \rightarrow a_2$ is Laporte forbidden in C_{2v} symmetry; therefore, $d_{x^2-y^2} \rightarrow d_{xy}$ would be formally forbidden and weak, consistent with the observed ϵ < 170 M^{-1} cm^{-1} for all the oxovanadium dithiolate complexes, with the notable exception of $[VO(tdt)_2]^{2-}$ (ϵ = 278 M^{-1} cm^{-1}). Here, due to the asymmetric nature of the anion, $[VO(tdt)_2]^{2-}$ is present in C_2 and C_s symmetry, and this transition becomes more allowed. However, the bands I and II are again assigned with a 7000 cm^{-1} difference in energy, in contrast with that of other VOX_4 and VOX_2Y_2 complexes. Low-temperature polarized single-crystal spectroscopy and low-temperature MCD spectroscopy of these reactive $[VOS_4]^{2-}$ anions may facilitate assignment of their electronic spectra. However, the low symmetry of these bis(chelate) complexes will make unique assignments difficult.[15]

The 77 K X-band EPR spectra of **1**−**3** are typical of near-axial d^1 V systems with hyperfine splitting from ^{51}V (I = $^7/_2$, 99.76% abundant). The spectra could be simulated with $g_{||} = 1.986$, $g_\perp = 1.989$, $A_{||} = 130.1 \times 10^{-4}$ cm^{-1}, and $A_\perp$ = 37.0 for **1**, $g_1 = 1.984$, $g_2 = 1.986$, $g_3 = 1.986$, $A_1 = 128.4$, $A_2 = 34.3$, and $A_3 = 38.3 \times 10^{-4}$ cm^{-1} for **2**, and g_1 = 1.985, $g_2 = 1.986$, $g_3 = 1.989$, $A_1 = 126.8$, $A_2 = 36.0$, and $A_3 = 32.4 \times 10^{-4}$ cm^{-1} for **3**. The g and A values are close to those reported for analogous complexes.[33,34,52,53,56,57] Recently, EPR has been used to study[58−60] the interaction

(54) Smith, P. D.; Cooney, J. J. A.; McInnes, E. J. L.; Beddoes, R. L.; Collison, D.; Harben, S. M.; Helliwell, M.; Mabbs, F. E.; Mandel, A.; Powell, A. K.; Garner, C. D. *J. Chem. Soc., Dalton Trans.* **2001**, 3108−3114.
(55) Kirk, M. L. Private communication, 2002.
(56) Matsubayashi, G.; Akiba, K.; Tanaka, T. *Inorg. Chem.* **1988**, *27*, 4744−4749.
(57) Marov, I. N.; Belyaeva, V. K.; Kalinichenko, N. B.; Mel'chakova, N. V.; Kirmse, R.; Dietsch, W.; Stach, J.; Hoyer, E. *Zh. Neorg. Khim.* **1986**, *31* (11), 2802−2810.

of oxovanadium complexes with ligands related to glutathione, which plays an important role in the biochemistry of vanadium.[61] The EPR parameters of compounds **1**−**3** are typical for oxovanadium(IV) compounds with four equatorial sulfur ligands.[58]

Molecular Orbital Calculations. The electronic structures of $[VO(bdt)_2]^{2-}$ and $[VO(bdtCl_2)_2]^{2-}$ were calculated using C_{2v} symmetry and in the absence of counterions. This results in the geometry-optimized structure being significantly different from the structure of the anion of **1** observed using X-ray crystallography. The ligating S atoms do not deviate from the basal plane of the square pyramid, consistent with C_{2v} geometry; this results in an O−V−S angle of 107.5° for $[VO(bdt)_2]^{2-}$ and 107.6° for $[VO(bdtCl_2)_2]^{2-}$. The V−S bonds are slightly longer (2.446 Å for $[VO(bdt)_2]^{2-}$ and 2.435 Å for $[VO(bdtCl_2)_2]^{2-}$); however, the remaining bond lengths are within ∓0.03 Å of the bond lengths found in the crystal structure. The C−Cl bonds are close to the literature value for aromatic C−Cl bonds (1.798 vs 1.739 Å).[62,63]

A qualitative molecular orbital diagram for $[VO(bdt)_2]^{2-}$ was derived from density functional calculations (see Figure S2). The ground-state electronic configuration for V in $[VO(bdt)_2]^{2-}$ is $3d^1$, and this unpaired electron resides in the $3d_{x^2-y^2}$-based molecular orbital, giving a doublet ground state, consistent with the EPR results. In the case of the spin-restricted (SR) calculation for the anion of $[VO(bdt)_2]^{2-}$ this MO is the singly occupied molecular orbital (SOMO). In the spin-unrestricted (SU) case the α-spin labeled MO is filled and the β-MO unoccupied. There is a large difference in energy between the highest ligand-based orbital ($23b_1$ HOMO: SR, 2.216 eV; α-SU, 2.229 eV; β-SU, 2.217 eV) and the lowest-energy virtual orbital ($30a_1$ LUMO: SR, 4.961 eV; α-SU, 4.894 eV; β-SU, 4.967 eV). The energies of the levels below the HOMO (symmetry-adapted linear combinations, SALCs) are very similar for the spin-restricted and unrestricted calculations. The SOMO, however, is at different energies for the spin-restricted and -unrestricted cases ($29a_1$ SOMO: SR, 3.141 eV; α-SU, 2.458 eV; β-SU, 4.012 eV). The SALCs consist of sulfur-based orbitals and can be assigned in a manner similar to those in $[MoOS_4]^-$,[15] with the four highest in energy as p_π and the next four as psuedo-σ.

The MO picture is very similar for $[VO(bdtCl_2)_2]^{2-}$ (see Figure S3), and there is a large difference in energy between the HOMO ($31b_1$: SR, 1.428 eV; α-SU, 1.441 eV; β-SU, 1.43 eV) and the LUMO ($38a_1$: SR, 4.146 eV; α-SU, 4.117 eV; β-SU, 4.194 eV). Also the SOMO is at different energies in the spin-restricted and -unrestricted cases ($37a_1$: SR, 2.374 eV; α-SU, 1.744 eV; β-SU, 3.201 eV). The four highest energy SALCs are p_π, and the next three are psuedo-σ. Two ligand-based orbitals occur above the remaining sulfur-based psuedo-σ orbital.

Table 4. Calculated Electronic Transitions for $[VO(bdt)_2]^{2-}$ and $[VO(bdtCl_2)_2]^{2-}$

	$[VO(bdt)_2]^{2-}$		$[VO(bdtCl_2)_2]^{2-}$	
transition	restricted	unrestricted	restricted	unrestricted
$b_1 \rightarrow a_1$ S $p\pi \rightarrow$ V $d_{x^2-y^2}$	12 372	14 953	11 872	14 340
$a_1 \rightarrow a_2$ $d_{x^2-y^2} \rightarrow d_{xy}$	15 582	17 131	16 196	17 881
$a_1 \rightarrow b_2$ $d_{x^2-y^2} \rightarrow d_{yz}$	17 074	18 478	16 873	18 575
$a_1 \rightarrow b_1$ $d_{x^2-y^2} \rightarrow d_{xz}$	17 801	19 228	18 301	19 817
$a_1 \rightarrow a_1$ $d_{x^2-y^2} \rightarrow d_{z^2}$	21 470	24 019	20 575	23 107
$a_1 \rightarrow b_2$ $d_{x^2-y^2} \rightarrow S_2\ 3p_z +$ $C_4\ 2p_z\ \pi(b_2)$	23 842	26 665	22 116	24 890

The electronic transitions for $[VO(bdt)_2]^{2-}$ and $[VO(bdtCl_2)_2]^{2-}$ are proposed as being either d → d transitions or LMCT.[1,33,34,51−53,56] Both of these types of transition involve the SOMO, which is the orbital whose energy is most dependent upon computational method (restricted vs unrestricted). Therefore, both types of calculation have been taken into account in analyzing the experimental electronic transitions. For $[VO(bdt)_2]^{2-}$ and $[VO(bdtCl_2)_2]^{2-}$ in both the spin-restricted and -unrestricted calculations the electronic transitions from $d_{x^2-y^2} \rightarrow d_{xy}$, d_{yz}, and d_{xz} are within 3000 cm^{-1}. The transition $d_{x^2-y^2} \rightarrow d_{z^2}$ is at higher energy. The ordering of $d_{x^2-y^2} < d_{xy} < d_{yz} < d_{xz} < d_{z^2}$ is the same as that seen for $[VOCl_4]^{2-}$. The energy of the LMCT is lower than those of the d → d transitions. It is important to note that the $d_{x^2-y^2} \rightarrow d_{xy}$ ($a_1 \rightarrow a_2$) transition is Laporte forbidden in C_{2v} symmetry; however, it may be accessible through geometric distortion of the anion to lower (C_2) symmetry or through vibronic coupling or spin−orbit coupling. The transition energies calculated in the spin-restricted mode are close to the observed values (see Tables 3 and 4). The respective energies calculated in spin-unrestricted mode are 1200−2600 cm^{-1} higher in energy; however, they follow the same trend. The values obtained are consistent with the assignment of the band at ∼11 000 cm^{-1} as a LMCT band, that at ∼17 500 cm^{-1} as $d_{x^2-y^2} \rightarrow d_{xy}$, d_{yz}, and d_{xz} bands overlapping, that at ∼20 000 cm^{-1} as $d_{x^2-y^2} \rightarrow d_{z^2}$, and that at 24 000 cm^{-1} as a MLCT band. However, the assignment of the band at ∼11 000 cm^{-1} as $d_{x^2-y^2} \rightarrow d_{xy}$ ($a_1 \rightarrow a_2$) cannot be discounted.

Conclusion

The synthesis of **1**−**3** was achieved via ligand substitution of $VO(acac)_2$ using the relevant proligand and triethylamine as a base. X-ray crystallography shows a "pseudo-C_2" structure for the anions of **1** and **2**. Triethylammonium cations are hydrogen-bonded to the anion, distorting the structure away from C_{2v} symmetry. The ammonium proton is hydrogen bonded to both a dithiolate sulfur and to the oxo group. These hydrogen-bonding interactions to sulfur and oxygen donor atoms mimic those found in the structures of pyranopterin enzymes.[7,9−11,37−45]

1−**3** show an electronic structure consistent with a d^1 V^{IV} center with a near-axial, five-coordinate, pseudo-square-

(58) Tasiopoulos, A. J.; Troganis, A. N.; Evangelou, A.; Raptopoulou, C. P.; Terzis, A. D. Y.; Kabanos, T. A. *Chem.—Eur. J.* **1999**, *5* (3), 910−921.
(59) Tasiopoulos, A. J.; Troganis, A. N.; Deligiannakis, Y.; Evangelou, A.; Kabanos, T. A.; Woollins, J. D.; Slawin, A. *J. Inorg. Biochem.* **2000**, *79*, 159−166.
(60) Jakusch, T.; Buglyó, P.; Tomaz, A. I.; Pessoa, J. C.; Kiss, T. *Inorg. Chim. Acta*, in press.
(61) Chasteen, N. D. *Struct. Bonding* **1983**, *53*, 105−138.
(62) Allen, H. A.; Olga, K.; Watson, D. G.; Brammar, L.; Orpen, A. G.; Taylor, R. *J. Chem. Soc., Perkin Trans. 2* **1987**, *S1*−*S19*.
(63) Kaftory, M. In *The Chemistry of Functional Groups. Supplement D: The Chemistry of Halides, Psuedohalides, and Azides*; Patai, S., Rappoport, Z., Eds.; Wiley: New York, 1983.

pyramidal geometry. The substituents on the 1,2-dithiolate ligand produce substantial changes in the V(V/IV) reduction potential, but the electronic absorption and EPR spectra of **1**−**3** are remarkably similar to those of other oxovanadium dithiolate anions.[1,33,34,51−53,56] Thus, even though the detailed assignment of the electronic absorption spectra of $[V^{IV}OS_4]^{2-}$ centers remains uncertain, it is clear that their overall electronic structure is maintained despite changes in the ligand periphery and structural distortions at the metal center induced by hydrogen-bonding interactions with the coordinated atoms. Hydrogen-bonding interactions are clearly important for anchoring the pyranopterindithiolate units themselves within enzymes. However, the hydrogen bonds to the terminal oxo groups and coordinated sulfur atoms of the metal atom may also play an important role in tuning the reactivity of these enzymes. This work has provided a simple mimic for such interactions.

Acknowledgment. We gratefully acknowledge partial support of this research by the NIH (Grant GM37773 to J.H.E.) and the NSF (Grant CHE9610374) for funds for the X-ray diffractometer. We thank Dr. F. E. Inscore and Dr. A. Raitsimring for helpful discussions.

Supporting Information Available: ORTEP representation of **2** and orbital energy diagrams showing the SALCs, the SOMO and LUMO derived from unrestricted and restricted DFT calculations. This material is available free of charge via the Internet at http://pubs.acs.org.

IC025856E